A Rapidly Convergent Nonlinear Transfinite Element Procedure for Transient Thermoelastic Analysis of Temperature-Dependent Functionally Graded Cylinders

M. Shariyat[*]

Faculty of Mechanical Engineering, K.N.T. University of Technology, Tehran, Iran

ABSTRACT

In the present paper, the nonlinear transfinite element procedure recently published by the author is improved by introducing an enhanced convergence criterion to significantly reduce the computational run-times. It is known that transformation techniques have been developed mainly for linear systems, only. Due to using a huge number of time steps, employing the conventional time integration methods requires quite huge computational time and leads to remarkable error accumulation, numerical instability, or numerical damping, especially for long investigation times. The present method specially may be extended to problems where the required time steps are of the order of the round-off errors (e.g., coupled thermoelasticty problems). The present procedure is employed for transient thermoelastic analysis of thick-walled functionally graded cylinders with temperature-dependent material properties, as an example. To reduce the effect of the artificial local heat and stress shock source generation at the mutual boundaries of the elements, second order elements are used. Influences of various parameters on the temperature and stress distributions are investigated. Furthermore, results of the proposed transfinite element technique are compared with the results obtained by other references to verify the validity, accuracy, and efficiency of the proposed method.

<div align="right">© 2009 IAU, Arak Branch. All rights reserved.</div>

Keywords: Nonlinear transfinite element; Transient thermoelastic analysis; Enhanced convergence; Functionally graded cylinders; Temperature-dependency

1 INTRODUCTION

ALTHOUGH the functionally graded materials (FGMs) are extensively employed to sustain elevated temperatures and severe temperature gradients, they have been mainly proposed to precisely monitor the distribution of the material properties within the stressed components to meet the local strength requirements. Extensive thermal stress studies made by Noda [1] and Tanigawa [2] reveal that due to continuously varying the volume fraction of the mixture of the materials, the huge local stresses and locally large plastic deformations, may be avoided or reduced in the FGM materials.

Among various FGM structures, cylindrical components have been of especial interest. Transient heat transfer analysis is a vital stage in development of strength investigations such as dynamic thermal buckling, fatigue life assessment under cyclic thermal loads, dynamic crack propagation, etc. Majority of the well-known heat transfer analyses performed so far for thick FGM cylinders are generally restricted to uniform heating [3] or steady state heat transfer [4-9] analyses. Some of these researches have been accomplished based on the multi-layered discretization approximation [10].

---

[*] Tel.: +98 912 272 7199; fax: +98 21 88674748.
  E-mail address: m_shariyat@yahoo.com and shariyat@kntu.ac.ir.

Some authors have investigated the transient heat transfer in isotropic cylinders [11-16]. Limited researches have been presented in the transient heat transfer analysis of the FGM cylinders. Furthermore, almost all of the presented researches have ignored the effect of the temperature-dependency of the material properties. Reddy and Chin [17] and Praveen et al. [18] have developed finite element formulations to analyze pseudo-dynamic thermoelastic responses of functionally graded cylinders subjected to abrupt thermal loadings. Obata et al. [19] analyzed the two-dimensional unsteady thermal stresses in an FGM hollow circular cylinder using the Laplace transformation and the perturbation method. Using the finite difference method, Awaji and Sivakumar [20] analyzed the steady-state and transient temperature distributions in an FGM cylinder. Based on the multi-layered cylinder approximation, Kim and Noda [21] studied the axisymmetric two dimensional transient thermoelasticity of an infinite FGM circular hollow cylinder using the Green's function method. Based on the local boundary integral equations with moving least square approximation of the temperature and heat flux, and using the numerical Laplace inversion method, Sladek et al. [22] studied the transient conduction heat transfer in the FGM cylinders. Wang et al. [23, 24] used the first order finite element method in conjunction with the finite-difference method to study the one dimensional transient heat conduction. Hosseini et al. [25], and Shao and Ma [26, 27] employed analytical methods to study the transient conduction heat transfer in FGM cylinders with material properties that follow an exponential law. Recently, thermo-mechanical analysis of FGM graded hollow circular cylinders subjected to linearly increasing boundary temperature is developed by Shao and Ma [27]. Thermo-mechanical properties of the functionally graded materials were assumed to be temperature independent. Hosseini [28] presented an analytical model for a functionally graded cylinder with finite length under thermal loads. He divided the cylinder into isotropic sub-cylinders and considered the material properties to be temperature-independent.

Almost in all of the above mentioned researches, the temperature-dependency of the material properties is neglected. Recently, a transient thermal analysis taking the temperature-dependency of the material properties into account is introduced by the author [29]. Time integration and an updating method were used. Only heat conduction was treated in the mentioned work. Majority of the finite element formulations presented in the heat transfer, thermal wave propagation or elastic wave propagation to date, are based on the first-order Lagrangian shape functions [17, 18, 23, 24, 30-33]. Since only C^0 continuity is guaranteed by Lagrangian elements, heat fluxes and stress components experience jumps at the mutual boundaries of the elements [34-36], especially when linear elements are used. Therefore, artificial sources of heat generation or concentrated tractions or wave sources will form at the mutual boundaries of the elements that in turn may remarkably influence the results. Some researchers has attempted to incorporate the kinematics and force conditions (Drichlet and Neumann boundary conditions) such as displacement and stress or temperature and flux conditions [33] (e.g., by modification of the generalized Hooke law). Generally, simultaneous incorporation of the mentioned types of boundary conditions may lead to some contradictions, such as altering the generalized Hooke's law or generation of heat sources or tractions at the mutual boundaries of the elements [36, 37].

In previous publications [38-41], the author and his coauthors have investigated the transient behaviors of cylinders undergoing thermomechanical dynamic or shock loads, taking the temperature-dependency of the material properties. The author has proposed the transfinite element method [38] for solving the time-dependent highly nonlinear problems, for the first time. In the present paper, the mentioned procedure is enhanced through employing a different convergence criterion. Convergence is a key issue in the nonlinear analyses that may significantly affect the computational run-times. Although the proposed method is very general and may be used for various branches of the science, nonlinear transient heat transfer and thermoelastic behavior of thick FGM cylinders with temperature-dependent material properties are investigated to clarify the proposed procedure. Second-order elements are used in the present research. In a thermal analysis problem, in contrast to stress analysis problems, changing the boundary condition type may lead to remarkable changes in the parametric form of the element matrices. In the present research, element matrices are dependent on both nodal and spatial coordinates.

The analytical technique which usually leads to a series solution, requires determination of a remarkable number of eigen values corresponding to mathematical expressions including different forms of complicated functions (e.g., Hankel's and Bessel's functions). Apart from the remarkable computational time required to determine the large number of the necessary eigen values and the corresponding eigen functions to obtain the prescribed accuracy, ignoring the higher eigen values may lead to losing effects of the higher modes whose effects are more noticeable in the early times of the transient responses. Furthermore, the analytical solutions are boundary condition dependent. So that changing the boundary conditions (e.g., thermal or stress boundary conditions), may lead to completely different eigen functions.

In some circumstances, the time integration methods may exhibit undesired responses such as: numerical oscillations, numerical damping, or numerical instability. These problems may arise due to improper choice of the integration time steps, the nature of the adopted numerical time integration scheme, and in nonlinear systems, the

updating procedure used and effect of the initial conditions and load values (e.g., thermal loads) on the frequencies and eigen values of the nonlinear system. Furthermore, since the integration time steps must be much less than the period time of the fundamental frequency of the system (e.g., of the order of 10^{-5} sec), both the accumulated errors and the computational times required to reach the final analysis time are remarkable.

In the present transfinite element method, much less computational time (about one tenth) is required in comparison with the analytical and the numerical time integration methods. The present solution algorithm prevents numerical oscillations and damping, and accumulated time integration errors and possesses the effect of all of the infinite eigen values of the analytical solution. Results of the present algorithm are compared with some results of the published well-known works. Finally, results based on the temperature-dependency and temperature-independency assumptions of the material properties are compared with each other and effects of various thermal boundary conditions are studied.

2   THE GOVERNING EQUATIONS

Geometric parameters of the thick-walled FGM cylinder are shown in Fig. 1. The FGM cylinder is assumed to be made of a mixture of two constituent materials so that the inner layer ($r = r_i$) of the cylinder is ceramic-rich, whereas the external layer $(r = r_o)$ is metal-rich.

Variation of the material properties with temperature may be expressed as follows [42, 43]:

$$P = P_0(1 + P_1 T + P_2 T^2 + P_3 T^3) \tag{1}$$

where P_0, P_1, P_2 and P_3 are some material constants. The material properties of the FGM cylinder at any arbitrary point through the thickness may be expressed based on the ceramic and metal material properties as [43]:

$$P = P_m + (P_c - P_m)\left(\frac{r_o - r}{r_o - r_i}\right)^N \tag{2}$$

c and m subscripts denote the ceramic and the metal properties, respectively. N is the so-called volume fraction index. Therefore, from Eqs. (1) and (2) one may conclude that:

$$P = P_{0m}(1 + P_{1m}T + P_{2m}T^2 + P_{3m}T^3) + [P_{0c}(1 + P_{1c}T + P_{2c}T^2 + P_{3c}T^3) - P_{0m}(1 + P_{1m}T + P_{2m}T^2 + P_{3m}T^3)]\left(\frac{r_o - r}{r_o - r_i}\right)^N \tag{3}$$

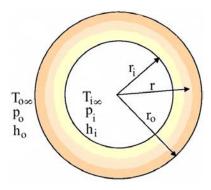The governing equation of the transient axisymmetric heat transfer problem is [44]

Fig. 1
Geometric parameters of the considered thick-walled FGM cylinder.

$$\frac{1}{r}\left[\frac{\partial T}{\partial r}\frac{\partial(\kappa r)}{\partial r}+\kappa r\frac{\partial^2 T}{\partial r^2}\right]-\rho C_v\frac{\partial T}{\partial t}=0 \tag{4}$$

where $\rho(r,T)$, $\kappa(r,T)$, and $C_v(r,T)$ are the mass density, the thermal conductivity, and the specific heat, respectively. Various thermal boundary conditions are considered in the present research:

a) An FGM cylinder with specified heat flux (e.g., due to passing hot gasses) at the inner surface and a convection heat transfer at the outer surface:

$$\begin{cases} \kappa\dfrac{\partial T}{\partial r}+h(T-T_\infty)=0 & at\ \ r=r_o \\ -\kappa\dfrac{\partial T}{\partial r}=q_o & at\ \ r=r_i \end{cases} \tag{5}$$

b) A sudden temperature increase at the inner surface and a convection heat transfer at the outer surface of the FGM cylinder:

$$\begin{cases} \kappa\dfrac{\partial T}{\partial r}+h(T-T_\infty)=0 & at\ r=r_o \\ T(r,t)=\overline{T}_i & at\ \ r=r_i \end{cases} \tag{6}$$

c) Thermal heat convection at both the internal and the external boundaries.
In all problems, it is assumed that all particles of the cylinder are initially at the ambient temperature:

$$T(r,0)=T_0 \tag{7}$$

Using a Kantorovich type approximation, variations of the temperature may be interpreted as [45]:

$$T(r,t)=\mathrm{N}(r)\mathrm{T}(t)^{(e)} \tag{8}$$

where $\mathbf{T}(t)^{(e)}$ is the nodal temperature values vector and N is the shape function matrix [45]:

$$\mathbf{N}=[\tfrac{1}{2}\xi(\xi-1)\quad(1-\xi^2)\quad\tfrac{1}{2}\xi(\xi+1)] \tag{9}$$

ξ is the natural coordinate. The relation between derivatives of the global and the natural coordinates is

$$\mathbf{N}_{,r}=\mathbf{N}_{,\xi}\xi_{,r}=\mathbf{N}_{,\xi}\frac{2n^{(e)}}{r_o-r_i}=\mathbf{N}_{,\xi}\frac{2}{\Delta r} \tag{10}$$

$n^{(e)}$ is number of elements. Using Galerkin's method, the governing equation of the element may be derived from the following equation:

$$\int_\Omega \mathrm{N}^{\mathrm{T}}R\,\mathrm{d}\Omega=0 \tag{11}$$

where

$$R = \rho C_v \mathbf{N} \dot{\mathbf{T}}^{(e)} - \frac{1}{r}\left[\mathbf{N}_{,r}\frac{\partial(\kappa r)}{\partial r} + \kappa r \mathbf{N}_{,rr}\right]\mathbf{T}^{(e)} \tag{12}$$

Therefore, the governing equation of the element will be

$$\mathscr{C}^{(e)}\dot{\mathbf{T}}^{(e)} + \mathscr{I}^{(e)}\mathbf{T}^{(e)} = \mathbf{Q}^{(e)} \tag{13}$$

Based on Eqs. (11) and (12), the damping matrix, $\mathscr{C}$, for all boundary conditions is

$$\mathscr{C}^{(e)} = \int_\Omega \rho C_v \mathbf{N}^{\mathrm{T}}\mathbf{N}\ \mathrm{d}\Omega \tag{14}$$

Matrices $\mathscr{C}$ and $\mathbf{Q}$ are different for various boundary conditions. For boundary condition type (a) one may write

$$\mathscr{I}^{(e)} = -\int_\Omega \mathbf{N}^{\mathrm{T}}\frac{1}{r}\frac{\partial(\kappa r)}{\partial r}\mathbf{N}_{,r}\ \mathrm{d}\Omega + \int_\Omega (\mathbf{N}^{\mathrm{T}}_{,r}\kappa + \mathbf{N}^{\mathrm{T}}\kappa_{,r})\mathbf{N}_{,r}\ \mathrm{d}\Omega + \int_{\Gamma_o}\mathbf{N}^{\mathrm{T}}h\mathbf{N}\ \mathrm{d}\Gamma_o$$
$$\mathbf{Q}^{(e)} = \int_\Gamma \mathbf{N}^{\mathrm{T}}\kappa\frac{\partial T}{\partial r}n_r\ \mathrm{d}\Gamma = \int_{\Gamma_i}\mathbf{N}^{\mathrm{T}}q_o\ \mathrm{d}\Gamma_i + \int_{\Gamma_o}\mathbf{N}^{\mathrm{T}}hT_\infty\ \mathrm{d}\Gamma_o \tag{15}$$

and for boundary condition type (b) one has

$$\mathscr{I}^{(e)} = -\int_\Omega \mathbf{N}^{\mathrm{T}}\frac{1}{r}\frac{\partial(\kappa r)}{\partial r}\mathbf{N}_{,r}\ \mathrm{d}\Omega + \int_\Omega (\mathbf{N}^{\mathrm{T}}_{,r}\kappa + \mathbf{N}^{\mathrm{T}}\kappa_{,r})\mathbf{N}_{,r}\ \mathrm{d}\Omega + \int_{\Gamma_o}\mathbf{N}^{\mathrm{T}}h\mathbf{N}\ \mathrm{d}\Gamma_o + \int_{\Gamma_i}\mathbf{N}^{\mathrm{T}}\kappa\mathbf{N}_{,r}\ \mathrm{d}\Gamma_i$$
$$\mathbf{Q}^{(e)} = \int_\Gamma \mathbf{N}^{\mathrm{T}}\kappa\frac{\partial T}{\partial r}n_r\ \mathrm{d}\Gamma = \int_{\Gamma_o}\mathbf{N}^{\mathrm{T}}hT_\infty\ \mathrm{d}\Gamma_o \tag{16}$$

where boundaries Γ_i and Γ_o are the inner and the outer surfaces of the cylinder, respectively. Eq. (15) may be used for the (c) type boundary conditions if similar boundary integrals with minus sign are added to account for the heat convection at the outermost layer of the FGM cylinder. The following relation is useful for calculation of the integrals appeared in Eqs. (15) and (16) numerically (using Gauss-Legendre method):

$$r = r_i + [2(e) + \xi - 1]\frac{\Delta r}{2} \tag{17}$$

e is the element number. Material properties and their derivatives may be calculated considereing the following identities:

$$T = \mathbf{N}(r)\mathbf{T}^{(e)}(t)$$
$$T^2 = \mathbf{T}(t)^{(e)\mathrm{T}}\mathbf{N}(r)^{\mathrm{T}}\mathbf{N}(r)\mathbf{T}(t)^{(e)}$$
$$T^3 = \mathbf{N}(r)\mathbf{T}(t)^{(e)}\mathbf{T}(t)^{(e)\mathrm{T}}\mathbf{N}(r)^{\mathrm{T}}\mathbf{N}(r)\mathbf{T}(t)^{(e)} \tag{18}$$

According to Eqs. (3) and (18), each material property is temperature-dependent (and subsequently, time dependent). Therefore, the element damping and stiffness matrices are temperature dependent. Therefore, the element matrices may be assembled to form the whole cylinder governing equations as

$$\mathscr{C}[\mathbf{T}(t)]\dot{\mathbf{T}}(t) + \mathscr{I}[\mathbf{T}(t)]\mathbf{T}(t) = \mathbf{Q}(t) \tag{19}$$

On the other hand, following the procedure outlined by the author in a previously published paper of the author [34], the governing equation of the elements may be expressed in the following form:

$$\mathscr{M}^{(e)}\ddot{\mathbf{U}}^{(e)} + \mathscr{K}^{(e)}\mathbf{U}^{(e)} = \mathscr{F}^{(e)} \tag{20}$$

where $\mathbf{U}^{(e)}$ is the nodal displacement vector. For a thermoelastic analysis where the internal and the external pressures of the cylinder are assumed to be zero, one has:

$$\mathscr{M}^{(e)} = \int_{\Omega} \rho[\mathrm{T}(t),\xi]\mathrm{N}^{\mathrm{T}}\mathrm{N}\,d\Omega \tag{21}$$

$$\mathscr{K}^{(e)} = \int_{\Omega} \mathrm{B}^{\mathrm{T}}\mathrm{D}[\mathrm{T}(t),\xi]\mathrm{B}\,d\Omega \tag{22}$$

$$\mathscr{F}^{(e)} = \int_{\Gamma_i} \mathrm{N}^{\mathrm{T}}p_i d\Gamma - \int_{\Gamma_o} \varepsilon\mathrm{N}^{\mathrm{T}}p_o\,d\Gamma + \int_{\Omega} \mathrm{B}^{\mathrm{T}}\mathrm{D}[\mathrm{T}(t),\xi]_{T}\,\Omega \tag{23}$$

where, for an axisymmetric cylinder experiences a plane strain field:

$$\boldsymbol{\varepsilon} = \begin{Bmatrix} \varepsilon_r \\ \varepsilon_\theta \end{Bmatrix} = \mathbf{dNU}^{(e)} = \mathbf{BU}^{(e)}, \qquad \mathbf{d} = \begin{bmatrix} \dfrac{\partial}{\partial r} \\ \dfrac{1}{r} \end{bmatrix} \tag{24}$$

$$\boldsymbol{\varepsilon}_T = \langle \alpha\Delta T \quad \alpha\Delta T \rangle \tag{25}$$

$$\boldsymbol{\sigma} = \mathbf{D}(\boldsymbol{\varepsilon} - \boldsymbol{\varepsilon}_T), \qquad \mathbf{D} = \frac{E(r)}{1 - v(r)^2}\begin{bmatrix} 1 & v(r) \\ v(r) & 1 \end{bmatrix} \tag{26}$$

Therefore, if the element matrices are assembled to construct the whole cylinder governing equations, one has:

$$\mathscr{M}[\mathbf{T}(\mathrm{t})]\ddot{\mathbf{U}}(t) + \mathscr{K}[\mathbf{T}(\mathrm{t})]\mathbf{U}(t) = \mathscr{F}(t) \tag{27}$$

3 THE PROPOSED NUMERICAL SOLUTION PROCEDURES

In a thermoelastic analysis, usually a two step solution is employed: (a) a thermal analysis; and (b) a stress analysis. In a time integration solution algorithm, this procedure is employed for each time step. Only the first analysis type (thermal analysis) is nonlinear.

3.1 The proposed numerical Laplace transform for the highly nonlinear governing equations

Using the Laplace transform definition

$$\mathrm{T}^*(s) = \mathscr{L}[\mathrm{T}(t)] = \int_0^\infty e^{-st}\mathrm{T}(t)\,dt \tag{28}$$

The system of the dynamic governing equations (19) may be reduced to a static one if $\mathscr{C}$, $\mathscr{I}$, and $\mathbf{Q}$ are assumed to be constant matrices. Since the material properties appeared in Eqs. (14) to (16) are temperature-dependent with the dependency defined in Eq. (3), $\mathscr{C}$, $\mathscr{I}$, and $\mathbf{Q}$ matrices are time dependent. Therefore, at the first glance, it may be deduced that a Laplace transform of a product of functions should be determined. A different procedure that is similar to using the tangential stiffness matrix concept in a traditional FEM updating procedure is used in the present paper. As a first stage, the matrices $\mathscr{C}$, $\mathscr{I}$, and $\mathbf{Q}$ are treated as constant matrices. In this regard, the initial values of the material properties are substituted into Eqs. (14) to (16). Therefore, if Eq. (19) is rewritten for the temperature increment:

$$\mathscr{E}\,\dot{\mathbf{\Theta}}(t) + \mathscr{I}\,\mathbf{\Theta}(t) = \widehat{\mathbf{Q}}(t) \tag{29}$$

where $\mathbf{\Theta} = \mathbf{T} - \mathbf{T}_0$ then the Laplace transform of Eq. (19) becomes:

$$(s\,\mathscr{E} + \mathscr{I})\mathbf{\Theta}^*(s) = \mathbf{Q}(s) \tag{30}$$

Boundary and initial condition equations may be incorporated in Eq. (30), in its transformed shape. The solution procedure continues in an iterative manner. In the first stage, the transformed temperature function is calculated from Eq. (30) as:

$$\mathbf{\Theta}^*(s) = (s\,\mathscr{E} + \mathscr{I})^{-1}\mathbf{Q}(s) \tag{31}$$

This temperature function may be used to update the material properties values according to Eq. (3) using the identities mentioned in Eq. (18).

The iterative solution that is intended to be proposed in this section is based on the ideas of the time integration procedure explained in the foregoing section but with a quite different concept. Material properties may readily be calculated if the nodal temperature values at any time instant are specified. Although the material properties are implicitly time-dependent, this dependency may be ignored in determining the material properties in an updating method. In other words, material properties may be defined in a parametric form, based on the temperature distribution obtained in the previous iteration. Therefore, Eq. (31) may be rewritten in the following form

$$\mathbf{\Theta}_i^*(s) = \left[s\,\mathscr{E}\big(\mathbf{\Theta}_{i-1}(t)\big) + \mathscr{I}\big(\mathbf{\Theta}_{i-1}(t)\big)\right]^{-1}\mathbf{Q}(s) \tag{32}$$

where

$$\mathbf{\Theta}(t) = \mathscr{L}^{-1}[\mathbf{\Theta}^*(s)] = \frac{1}{2\pi i}\int_{\vartheta-i\infty}^{\vartheta+i\infty} e^{st}\,\mathbf{\Theta}^*(s)\,ds \tag{33}$$

is the inversion of the Laplace transform of the nodal temperature vector. $i = \sqrt{-1}$ is the unit imaginary number and ϑ is an arbitrary real value that is greater than all real parts of the singularities of $\mathbf{\Theta}^*(s)$ components.

Following a method proposed by Honig and Hirdes [47], numerical inversion of the Laplace transform can be written as

$$\mathbf{\Theta}(t) \cong \tfrac{1}{2}\,\mathscr{A}_0 + \sum_{k=1}^{n}\mathscr{A}_k \tag{34}$$

$$\mathscr{A}_k = \frac{e^{\vartheta t}}{\tau}\left\{ \mathrm{Re}\left[\mathbf{\Theta}^*(\vartheta + i\frac{k\pi}{\tau})\right]\cos\frac{k\pi t}{\tau} - \mathrm{Im}\left[\mathbf{\Theta}^*(\vartheta + i\frac{k\pi}{\tau})\right]\sin\frac{k\pi t}{\tau} \right\}, \quad k = 0,1,2,... \tag{35}$$

It may be noted that a good choice of the arbitrary parameters n, ϑ, and τ is not only important to enhance the accuracy of the results but also crucial for the application of the Korrektur method [47] and the methods proposed to accelerate the convergence. Values of ϑ and τ are chosen according to criteria outlined by Honig and Hirdes in reference [47]. In the Korrectur method the optimal value of ϑ is found for any fixed values of n and τ, by minimization of the sum of the absolute values of the discretization and truncation errors [47].

If after some iterations, both $\mathrm{Re}\left[\mathbf{\Theta}^*(\vartheta + i\frac{k\pi}{\tau})\right]$ and $\mathrm{Im}\left[\overset{*}{\mathbf{\Theta}}(\vartheta + i\frac{k\pi}{\tau})\right]$, $(k = 0,...,n)$ become negligibly small, it

may be concluded that the solution is obtained with a sufficient accuracy. Therefore, since $\mathbf{\Theta}^*$ is dependent on both r and s variables, the following convergence criterion may be used in this regard:

$$\max_{k,j}\left(\frac{\left\|\mathrm{Re}\left(\overset{*}{\Theta}_m(\vartheta+i\frac{k\pi}{\tau})-\overset{*}{\Theta}_{m-1}(\vartheta+i\frac{k\pi}{\tau})\right)\right\|}{\left\|\mathrm{Re}\left(\overset{*}{\Theta}_m(\vartheta+i\frac{k\pi}{\tau})\right)\right\|}\ ,\ \frac{\left\|\mathrm{Im}\left(\overset{*}{\Theta}_m(\vartheta+i\frac{k\pi}{\tau})-\overset{*}{\Theta}_{m-1}(\vartheta+i\frac{k\pi}{\tau})\right)\right\|}{\left\|\mathrm{Im}\left(\overset{*}{\Theta}_m(\vartheta+i\frac{k\pi}{\tau})\right)\right\|}\right)\le\ \in,\qquad j=1,\ldots,n^* \tag{36}$$

where *m* is the iteration counter, *j* is the node number, n^* is the number of nodes, and $\in$ is a prescribed sufficiently small value (e.g., 0.001). It is obvious that when convergence is achieved, values of the material properties will be in agreement with the resulted temperature distribution. In the previously published work of the author [38], the convergence criterion has been proposed to be checked in the time domain.

3.2 The proposed numerical procedure for the thermoelastic analysis

Thermoelastic stresses are calculated based on the converged temperature distribution. In this regard, the transformed form of Eq. (27) is used:

$$\left\{s^2\mathcal{M}[\mathbf{T}^*(s)]+\mathcal{K}[\mathbf{T}^*(s)]\right\}\mathbf{U}^*(s)=\mathcal{F}(s) \tag{37}$$

or

$$\mathbf{U}^*(s)=\left\{s^2\mathcal{M}[\mathbf{T}^*(s)]+\mathcal{K}[\mathbf{T}^*(s)]\right\}^{-1}\mathcal{F}(s) \tag{38}$$

Time variations of the nodal radial displacements may be determined using a numerical Laplace inversion similar to Eq. (34) [46]:

$$\tag{39}$$

$$\mathbf{U}(t)\cong\tfrac{1}{2}\mathcal{B}_0+\sum_{k=1}^n\mathcal{B}_k$$

$$\mathcal{B}_k=\frac{e^{\vartheta t}}{\tau}\left\{\mathrm{Re}\left[\mathbf{U}^*(\vartheta+i\frac{k\pi}{\tau})\right]\cos\frac{k\pi t}{\tau}-\mathrm{Im}\left[\mathbf{U}^*(\vartheta+i\frac{k\pi}{\tau})\right]\sin\frac{k\pi t}{\tau}\right\},\quad k=0,1,2,\ldots \tag{40}$$

Time variations of the stress components may be determined by substituting $\mathbf{U}(t)$ into Eq. (24) and substituting the resulted equation into Eq. (26).

4   RESULTS AND DISCUSSIONS

A sensitivity analysis has been carried out to determine the proper number of elements and the suitable time itegration steps. Number of elements is so chosen that almost no difference is noticed in the results by using a finer mesh. Since the transfinite element procedure requires a parametric (symbolic) analysis, the computer program is written in MATLAB and Maple softwares environments.

As a validation example, an FGM hollow cylinder of reference [24] whose inner and outer radii are 50 and 150 (mm), respectively is considered. The material phases inside the FGM cylinder change from pure ZrO_2 at the outermost layer linearly to Ti–6Al–4V at the innermost layer. The inner surface of the cylinder is suddenly heated to $T_i=1000\ \mathrm{K}$; which is maintained thereafter. Temperature of the outer surface of the cylinder is kept zero. The properties of ZrO_2 and Ti–6Al–4V materials are similar to those mentioned in reference [24]. The simple rule-of-mixture is applied to evaluate the overall property distribution of the FGM. The temperature distributions predicted by reference [24] are compared with those obtained using the present algorithm in Fig. 2, for both temperature-dependent (TD) and temperature-independent (TID) material properties. According to Fig. 2, generally, there is an agreement between the results. Greater discrepancies are noticed in prediction of behaviors of FGM cylinders with temperature-dependent materials. Results of reference [24] are derived based on linear elements in conjunction with
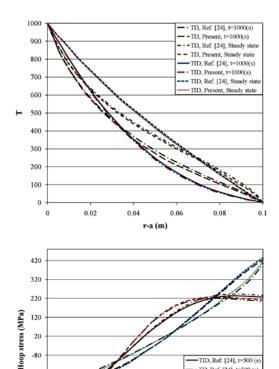
Fig. 2
A comparison between the predicted behaviors of FGM cylinders with temperature-dependent (TD) and temperature-independent (TID) material properties.

Fig. 3
A comparison among the predicted hoop stresses of FGM cylinders with temperature-dependent (TD) and temperature-independent (TID) material properties.

the finite difference method (instead of the iterative solution procedure). Although the results show a good agreement, using linear elements to predict nonlinear variations (especially in a stress analysis) may lead to abrupt changes in derivatives of the nodal values at the boundaries of the elements and may lead to remarkable errors in the results [34, 35]. However, the greater discrepancies are noticed in smaller times where the transient effects are more pronounced. For FGM cylinders with temperature-dependent material properties, the temperature distribution curves have inflection points. Besides, it is an evident that the influence of the temperature-dependency of the material properties grows with the temperature. The transient hoop stress distributions are shown in Fig. 3. Results of reference [24] are derived through using relations that govern the static behavior of the isotropic cylinders. Therefore, the inertia effects are ignored. It is known that results obtained through modeling the nonlinear systems by means of Lagrangian elements may have noticeable errors in the neighborhoods of the boundaries [34, 35] as it may be seen in Fig. 3. Furthermore, in contrast to second order finite element formulation, first order finite element formulation increases the compliance of the system [35]. For this reason, the magnitudes of the stress values of reference [24] are somewhat lower.

As a second example, effects of the temperature-dependency of the material properties on the temperature distribution are considered. To this end, a thick-walled Ti-6Al-4V/Si_3N_4 FGM cylinder with the following geometric and heat transfer data are considered:

$$r_i = 12.7 \, mm, \qquad r_o = 25.4 \, mm, \qquad T_i = 450 \, K, \qquad Q_0 = 1000 \, kw/m^2, \qquad h = 8 \, wK/m^2$$

Material properties are given in Table 1 [17]. Results are expressed in terms of the dimensionless radius, radius ratio, and dimensionless time defined as:
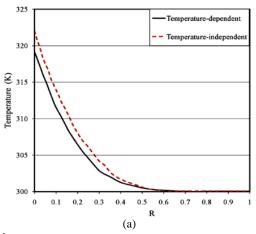
$$R = \frac{r - r_i}{r_o - r_i} \, , \qquad \overline{R} = \frac{r_i}{r_o} \, , \qquad \overline{t} = \frac{t}{\tau} \tag{41}$$

Table 1
Material properties of the considered FGM cylinder [17]

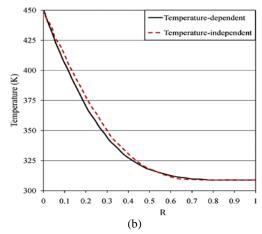| Property	Coefficient	Metal (Ti-6Al-4V)	Ceramic ((Si_3N_4))
κ (W / mK)	P_0	1.20947	13.723
	P_1	0.0139375	0
	P_2	0	0
	P_3	0	0
ρ (kg / m^3)	P_0	2370	4429
	P_1	4429	2370
	P_2	0	0
	P_3	0	0
	P_0	0	0
α (K^{-1})	P_1	7.57876e-6	5.8723e-6
	P_2	0	0
	P_3	0.00065	9.095 e -4
	P_0	0.313467 e -6	0
	P_1	0	0
C_v (J / kgK)	P_2	625.29692	555.11
	P_3	0	0
	P_0	-4.2238757e-4	1.016e-3
	P_1	7.1786536e-7	2.92e-7
	P_2	0	-1.67e-10

Fig. 4
A comparison between results of temperature-dependent and temperature-independent thick-walled FGM cylinders (N=1, $\bar{t} = 0.2, \bar{R} = 2$) for: (a): boundary condition type *a* and (b): boundary condition type *b*.

Influence of the temperature-dependency on the temperature distribution of FGM cylinders is depicted in Fig. 4 for (N=1, $\bar{t} = 0.2, \bar{R} = 2$). As it may be noticed from Fig. 4, higher temperatures and temperature gradients are resulted when the temperature-dependency of the material properties is ignored (it was discussed in relation to Fig. 2). A difference up to 15 percent in ΔT is observed in the results of the first type of the boundary conditions. Since

temperature values increase with time, this difference is more remarkable for greater values of the dimensionless time ($\bar{t}$). Therefore, if the temperature distributions predicted based on the temperature-independent material properties assumption are used in a strength analysis of an FGM Cylinder with temperature-dependent material properties, lower strength values will result. Therefore, the materials will not be adequately utilized.

Finally, temperature, radial displacement, radial stress, and hoop stress transient responses of a thick-walled SUS304/Si_3N_4 cylinder with the following specifications are investigated for the first 10(s) time interval:
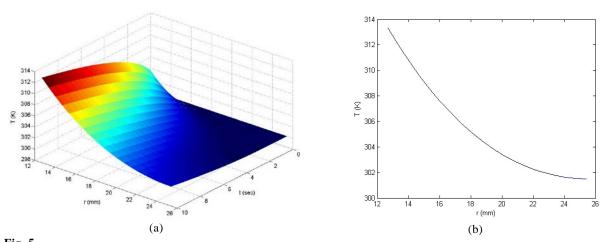
$$r_i = 12.7\,mm, \qquad r_o = 25.4\,mm, \qquad N = 1$$

The internal layer of the cylinder is ceramic-rich. Coefficients of Eq. (3) of the constituent materials are extracted from Reddy and Chin [17]. They are not mentioned here to save space. It is assumed that the cylinder is initially at the ambient temperature (300 K). Both internal and external boundaries of the cylinder are subjected to a convection heat transfer with the following parameters:

$$h = 100\,wK/m^2, \qquad T_{i\infty} = 600\,K, \qquad T_{o\infty} = 300\,K$$

According to a preliminary frequency analysis, it was found that the period time corresponding to the fundamental natural frequency of the cylinder is in the order of 10^{-5} s . Therefore, if a time integration solution procedure is used, a time step in the order of 10^{-6} s should be used. Therefore, a considerable computational time would be required and accumulated errors will be resulted. Hence, once again the efficiency of the proposed algorithm is confirmed. In Figs. 5 to 8, the distribution of the temperature, the radial displacement, the radial stress, and the hoop stress versus time and radius as well as the distribution for t=10 (s) are illustrated for the considered FGM cylinder. In Fig. 6, as it may be expected, positive radial displacements have been occurred. As it may be expected, the inner layer has a less freedom to expand in the radial direction than the outer free layer (especially when it is fabricated from a ceramic material as it is the case in the present example). On the other hand, all the internal expansions influence the expansion of the free outer layer. Since the inner layers experience higher temperatures, the maximum radial displacement has occurred in an intermediate layer.

As Fig. 7 shows, due to the tendency of the layers to move outward for the given boundary conditions, a compressive radial stress distribution has been formed whose extremum has occurred in an intermediate layer (which is closer to the inner layer, in comparison with the outer layer). On the other hand, as Fig. 8 implies, due to expansion of the layers, a tensile hoop stress distribution has appeared. It is evident that for the present boundary conditions, the expansions and subsequently the hoop stresses are more remarkable for the internal layers. Figs. 6(a), 7(a) and 8(a) show small local oscillations in the displacement and stress responses due to the transient nature of the responses.

(a)   (b)

Fig. 5.
Transient temperature distribution of the SUS304/Si_3N_4 cylinder: (a) the transient time variation of the distribution and (b) the distribution for t=10 (s).
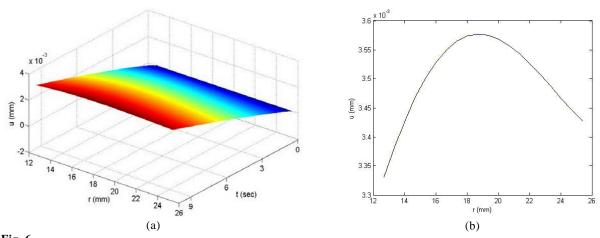
Fig. 6
 Transient radial displacement distribution of the SUS304/ Si$_3$N$_4$ cylinder: (a) the transient time variation of the distribution and (b) the distribution for *t*=10 (s).
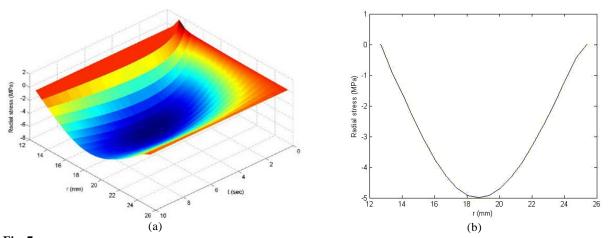

Fig. 7.
Transient radial stress distribution of the SUS304/ Si$_3$N$_4$ cylinder: (a) the transient time variation of the distribution and (b) the distribution for *t*=10 (s).
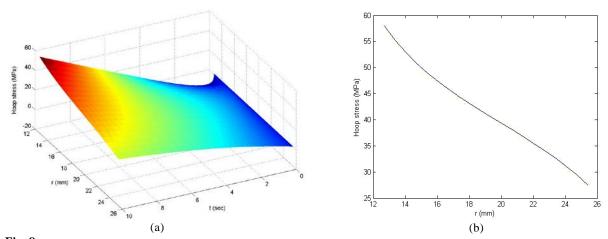

Fig. 8.
Transient hoop stress distribution of the SUS304/ Si$_3$N$_4$ cylinder: (a) the transient time variation of the distribution and (b) the distribution for *t*=10 (s).

5   CONCLUSIONS

In the present paper, nonlinear transient heat transfer and thermoelastic behaviors of the thick-walled FGM cylinders are investigated by a transfinite element method that may be used in an updating and iterative solution scheme. The main novelties of the present research are: (1) incorporating the temperature-dependency of the material properties in the thermal analysis, (2) proposing a numerical transfinite element procedure that may be used in a Picard iterative algorithm to update the material properties in a highly nonlinear formulation, and (3) employing an adequate convergence criterion.

Remarkable computational time is required to determine the large number of the necessary eigen values and the corresponding eigen functions in the analytical techniques to obtain the prescribed accuracy. Besides, ignoring the higher eigen values may lead to losing effects of the higher modes whose effects are more noticeable in the early times of the transient responses. Furthermore, the analytical solutions are boundary condition dependent. So that changing the boundary conditions (e.g., thermal or stress boundary conditions), may lead to completely different eigen functions. On the other hand, the time integration methods may exhibit undesired responses such as: numerical oscillations, numerical damping, or numerical instability [36]. These problems may arise due to improper choice of the integration time steps, the nature of the adopted numerical time integration scheme, and in nonlinear systems, the updating procedure used and the initial conditions and load values (e.g., thermal loads) on the frequencies and eigenvalues of the nonlinear system. Furthermore, since the integration time steps must be much less than the period time of the fundamental frequency of the system (e.g., of the order of 10^{-5} sec), both the accumulated errors and the compilation times required to reach the final analysis time are remarkable.

In the present transfinite element method, much less computational time (about one tenth) is required in comparison with the analytical and the numerical time integration methods. Furthermore, accumulated time integration errors and numerical oscillations, damping or instability are avoided in the proposed transfinite element technique. Besides, in contrast to researches developed so far, second order elements are employed. Therefore, the proposed transfinite element method may be adequately used in problems where time integration method is not recommended because of truncation errors (e.g., coupled thermoelasticity problems with very small relaxation times) or where improper choice of the time integration step may lead to loss of the effects of the higher mode functions in the dynamic response. Besides, analytical solutions are not available for general cases. Generally, determining the eigen values and the associated eigen functions that usually requires solving equations expressed in terms of Hankel or Bessel functions, is cumbersome. Therefore, it seems that the present technique may be used to obtain relatively accurate and stable results in a less computational time. Results also show that the temperature-dependency of the material properties may significantly affect the temperature and subsequently, the stress distribution that have remarkable effects on some critical behaviors such as thermal buckling or dynamic crack propagation phenomena.

RFERENCES

[1]   Noda N., 1991, Thermal stresses in materials with temperature-dependent properties, *ASME Applied Mechanics Review* **44**: 83-97.
[2]   Tanigawa Y., 1995, Some basic thermoelastic problems for non-homogeneous structural materials, *ASME Applied Mechanics Review* **48**: 287-300.
[3]   Zimmerman R.W., Lutz M.P., 1999, Thermal stress and thermal expansion in a uniformly heated functionally graded cylinder, *Journal of Thermal Stresses* **22**: 88-177.
[4]   Obata Y., Noda N., 1994, Steady thermal stresses in a hollow circular cylinder and a hollow sphere of a functionally gradient material, *Journal of Thermal Stresses* **17**: 471-487.
[5]   El-abbasi N., Meguid S.A., 2000, Finite element modeling of the thermoelastic behavior of functionally graded plates and shells, *International Journal of Computational Engineering Science* **1**: 51-165.
[6]   Jabbari M., Sohrabpour, S. Eslami M.R., 2001, Mechanical and thermal stresses in a functionally graded hollow cylinder due to radially symmetric loads, *International Journal of Pressure Vessels and Piping* **79**: 493-497.
[7]   Liew K.M., Kitipornchai S., Zhang X.Z., Lim C.W., 2003, Analysis of the thermal stress behavior of functionally graded hollow circular cylinders, *International Journal of Solids and Structures* **40**: 2355-2380.
[8]   Jabbari M., Sohrabpour S., Eslami M.R., 2003, General solution for mechanical and thermal stresses in a functionally graded hollow cylinder due to nonaxisymmetric steady-state loads. *ASME Journal of Applied Mechanics* **70**: 111-118.
[9]   Ching H.K., Yen S.C., 2005, Meshless local Petrov-Galerkin analysis for 2D functionally graded elastic solids under mechanical and thermal loads, *Composites Part B: Engineering* **36**: 223-240.

[10] Wang X., 1995, Thermal shock in a hollow cylinder caused by rapid arbitrary heating, *Journal of Sound and Vibration* **183**(5): 899-906.

[11] Kandil A., EL-Kady A.A., EL-Kafrawy A., 1995, Transient thermal stress analysis of thick-walled cylinders, *International Journal of Mechanical Sciences* **37**: 721-732.

[12] Segall A.E., 2003, Transient analysis of thick-walled piping under polynomial thermal loading, *Nuclear Engineering and Design* **226**: 183-191.

[13] Segall A.E., 2004, Thermoelastic stresses in an axisymmetric thick-walled tube under an arbitrary internal transient, *ASME Journal of Pressure Vessel Technology* **126**: 327-332.

[14] Lee Z.Y., 2005, Hybrid numerical method applied to 3-D multilayered hollow cylinder with periodic loading conditions, *Applied Mathematics and Computation* **166**: 95-117.

[15] Shahani A.R., Nabavi S.M., 2007, Analytical solution of the quasi-static thermoelasticity problem in a pressurized thick-walled cylinder subjected to transient thermal loading, *Applied Mathematical Modelling* **31**: 1807-1818.

[16] Ramadan K., 2009, Semi-analytical solutions for the dual phase lag heat conduction in multilayered media, *International Journal of Thermal Sciences* **48**(1): 14-25.

[17] Reddy J.N., Chin C.D., 1998, Thermomechanical analysis of functionally graded cylinders and plates, *Journal of Thermal Stresses* **21**: 593-626.

[18] Praveen G.N., Chin C.D., Reddy J.N., 1999, Thermoelastic analysis of a functionally graded ceramic-metal cylinder, *ASCE Journal of Engineering Mechanics* **125**(11): 1259-1267.

[19] Obata Y., Kanayama K., Ohji T., Noda N., 1999, Two-dimensional unsteady thermal stresses in a partially heated circular cylinder made of functionally gradient materials, in: *3rd International Congress on Thermal Stresses*, 595-598.

[20] Awaji H., Sivakumar R., 2001, Temperature and stress distribution in a hollow cylinder of functionally graded material: the case of temperature-independent material properties, *Journal of the American Ceramic Society* **84**: 1059-1065.

[21] Kim K.S., Noda N., 2002, Green's function approach to unsteady thermal stresses in an infinite hollow cylinder of functionally graded material, *Acta Mechanica* **156**: 145-61.

[22] Sladek J., Sladek V., Zhang C., 2003, Transient heat conduction analysis in functionally graded materials by the meshless local boundary integral equation method, *Computational Materials Science* **28**: 494-504.

[23] Wang B.L., Mai Y.W., Zhang X.H., 2004, Thermal shock resistance of functionally graded materials, *Acta Materialia* **52**: 4961-4972.

[24] Wang B.L., Mai Y.W., 2005, Transient one-dimensional heat conduction problems solved by finite element, *International Journal of Mechanical Sciences* **47**: 303-317.

[25] Hosseini S.M., Akhlaghi M., Shakeri M., 2007, Transient heat conduction in functionally graded thick hollow cylinders by analytical method, *Heat and Mass Transfer* **43**: 669-675.

[26] Shao Z.S., Wang T.J., Ang K.K., 2007, Transient thermo-mechanical analysis of functionally graded hollow circular cylinders, *Journal of Thermal Stresses* **30**(1): 81-104.

[27] Shao Z.S., Ma G.W., 2008, Thermo-mechanical stresses in functionally graded circular hollow cylinder with linearly increasing boundary temperature, *Composite Structures* **83**(3): 259-265.

[28] Hosseini S.M., 2009, Coupled thermoelasticity and second sound in finite length functionally graded thick hollow cylinders (without energy dissipation), *Materials & Design* **30**(6): 2011-2023.

[29] Shariyat M., 2008, Dynamic thermal buckling of suddenly heated temperature-dependent FGM cylindrical shells, under combined axial compression and external pressure, *International Journal of Solids and Structures* **45**: 2598-2612.

[30] He T., Tian X., Shen Y., 2002, Two-dimensional generalized thermal shock problem of a thick piezoelectric plate of infinite extent, *International Journal of Engineering Science* **40**: 2249-2264.

[31] Tian X., Shen Y., Chen C., He T., 2006, A direct finite element method study of generalized thermoelastic problems, *International Journal of Solids and Structures* **43**: 2050-2063.

[32] Bagri A., Eslami M.R., 2008, Generalized coupled thermoelasticity of functionally graded annular disk considering the Lord–Shulman theory, *Composite Structures* **83**(2): 168-179.

[33] Shakeri M., Akhlaghi M., Hoseini S.M., 2006, Vibration and radial wave propagation velocity in functionally graded thick hollow cylinder, *Composite Structures* **76**: 174-181.

[34] Shariyat M., Eslami M.R., 1996, Isoparametric finite-element thermoelasto-plastic creep analysis of shells of revolution, *International Journal of Pressure Vessels and Piping* **68**(3): 249-259.

[35] Zienkiewicz O.C., Taylor R.L., 2005, *The Finite Element Method: Its Basis and Fundamentals,* Butterworth-Heinemann, 6th edition.

[36] Reddy J.N., 2005, *An Introduction to the Finite Element Method*, McGraw-Hill, 3rd edition.

[37] Heinrich J.C., Pepper D.W., 2005, *The Finite Element Method: Basic Concepts and Applications*, Taylor & Francis, 2nd edition.

[38] Shariyat M., 2009, A nonlinear Hermitian transfinite element method for transient behavior analysis of hollow functionally graded cylinders with temperature-dependent materials under thermo-mechanical loads, *International Journal of Pressure Vessels and Piping* **86**: 280-289.

[39] Shariyat M., Lavasani S.M.H., Khaghani M., 2010, Nonlinear transient thermal stress and elastic wave propagation analyses of thick temperature-dependent FGM cylinders, using a second-order point-collocation method, *Applied Mathematical Modelling*, doi: 10.1016/j.apm.2009.07.007.

[40] Shariyat M., Khaghani M., Lavasani S.M.H., 2010, Nonlinear thermoelasticity, vibration, and stress wave propagation analyses of thick FGM cylinders with temperature-dependent material properties, *European Journal of Mechanics-A/Solids*, doi: doi:10.1016/j.euromechsol.2009.10.007.

[41] Azadi M., Shariyat M., 2009, Nonlinear transient transfinite element thermal analysis of thick-walled FGM cylinders with temperature-dependent material properties. *Meccanica*, doi: 10.1007/s11012-009-9249-4.

[42] Shen H.-S., 2009, *Functionally Graded Materials: Nonlinear Analysis of Plates and Shell,* CRC Press, Taylor & Francis Group, Boca Raton.

[43] Touloukian Y.S., 1976, *Thermophysical Properties of High Temperature Solid Materials*, McMillan, New York.

[44] Hetnarski R.B., Eslami M.R., 2009, *Thermal Stresses - Advanced Theory and Applications*, Springer.

[45] Reddy, J.N., 2005, *An Introduction to the Finite Element Method*, 3rd edition, McGraw-Hill.

[46] Honig G., Hirdes U., 1984, A method for the numerical inversion of Laplace transforms, *Journal of Computational and Applied Mathematics* **10:** 113-132.